J|A|C|S
COMMUNICATIONS

Published on Web 03/03/2006

Single-Molecule Force Spectroscopy of Bimolecular Reactions: System Homology in the Mechanical Activation of Ligand Substitution Reactions

Farrell R. Kersey, Wayne C. Yount, and Stephen L. Craig*

Department of Chemistry and Center for Biologically Inspired Materials and Material Systems, Duke University, Durham, North Carolina 27708-0346

Received December 15, 2005; E-mail: stephen.craig@duke.edu

Single-molecule force spectroscopy (SMFS) provides access to details of molecular mechanics and features of potential energy landscapes that hitherto have been inaccessible. SMFS studies have included, but are not limited to, protein folding pathways,[1] unimolecular isomerization,[2] conformational changes within polymers,[3] and intermolecular forces,[4] including metal−ligand bonds.[4e−h] SMFS also holds promise as a mechanistic probe for studying bimolecular potential energy surfaces, and we report here that the mechanical activation of a leaving group accelerates nucleophilic substitution of dimethyl sulfoxide (DMSO) for substituted pyridines at square-planar pincer Pd(II) metal centers.[5] The mechanical responses of a pair of reactions are homologous and scale with the rates of the unactivated reactions.

The experimental design is shown schematically in Figure 1. Pyridine ligands **2** were attached to both an AFM tip and a SiO_2 substrate by coupling to the terminal amine of surface-tethered PEGs (MW ∼ 3400 g/mol), a strategy that has been shown to be useful in placing specific rupture events outside the range of nonspecific adhesion.[4e,f,6] The surface chemistry, combined with the introduction of a DMSO solution of bifunctional metal complex **1**, provides an opportunity for bridging bond formation of the type shown in Figure 1. At appropriate concentrations of **1**, such events are thermodynamically (equilibrium constants ∼1300 and 30 M^{-1} for **2a** and **2b**, respectively) and kinetically (time scale of bond formation < seconds) accessible.[7]

When the tip and surface, both functionalized with **2a**, are brought into contact in DMSO and then withdrawn, only nonspecific contact adhesion is observed in the force-extension curves; no interactions involving adhesion other than single PEG stretching (<25 nm) are detectable. When 0.86 mM **1** is introduced, however, specific bond rupture events are recorded at extensions centered at ∼43 nm, consistent with the expected length of two PEG tethers (∼25 nm each), as shown in Figure 2a. The features are consistent with the rupture of single-molecule bridging events of the type shown in Figure 1. Support for the predominance of single-molecule events comes from competitive inhibition of the **1**·$(\mathbf{2a})_2$ complex, in which 100 mM 4-(dimethylamino)pyridine (DMAP) is added to the DMSO solution of **1**. Under these inhibition conditions, the same specific rupture events were observed, but with much less frequency: ∼10% of force-extension curves before addition of DMAP, compared to ∼3% after addition of DMAP. A similar treatment was carried out for system **1**·$(\mathbf{2b})_2$, where 100 mM of added pyridine reduced the frequency of specific events from 16 to 5%.

Histograms were created from the force-extension curves (corrected for viscous drag) to obtain the most probable rupture force, derived from Gaussian fits to the distribution profiles. Rupture events observed at extensions between 20 and 100 nm were used in the data analysis; the distribution in extensions at rupture is attributed to off-angle attachments and the coupling of some ligands

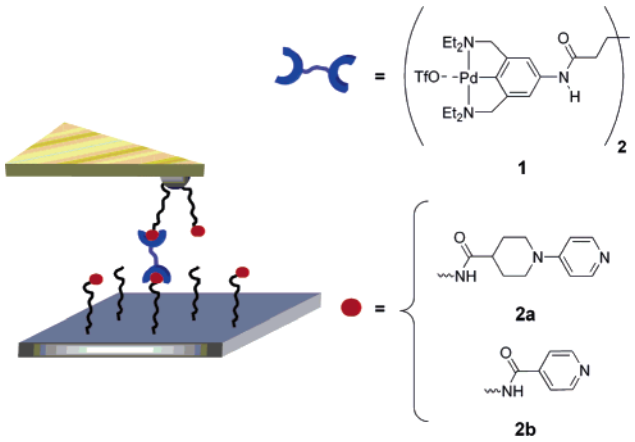

Figure 1. Schematic representation of a single-molecule force spectroscopy experiment. Poly(ethylene glycol) linkers were attached to an AFM tip and substrate and subsequently functionalized with either **2a** or **2b**. A DMSO solution of **1** was added between the tip and surface to carry out experiments.

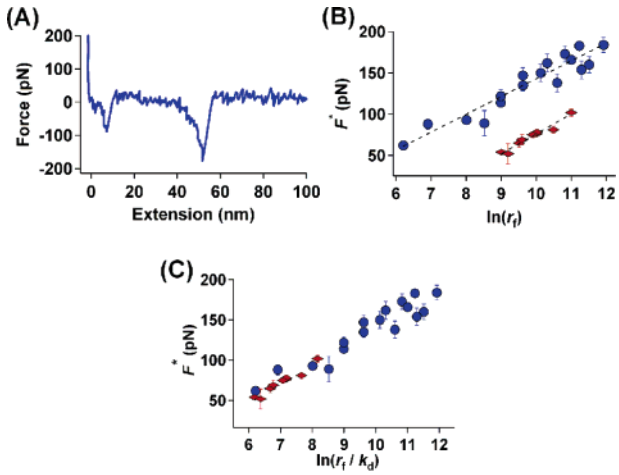

Figure 2. (A) A representative force-separation curve showing bond rupture in **1**·$(\mathbf{2a})_2$ during retraction of the AFM tip. (B) Most probable force versus loading rate of the **1**·$(\mathbf{2a})_2$ (●) and **1**·$(\mathbf{2b})_2$ (◆) coordination systems (see Supporting Information for details). Error bars reflect the standard error ($\sigma/\sqrt{N}$) of Gaussian fits to the distributions. (C) Master graph of force versus loading rate scaled by thermal dissociation rates k_{diss} measured independently by NMR. Data were acquired on multiple days with different cantilevers.

to the surface either directly or through sequentially coupled polymers. Nonetheless, forces are largely independent of extension at rupture (Supporting Information), and the use of a narrower range of extensions (e.g., 30−60 nm) does not appreciably affect the results. The most probable rupture force reflects a competition between force loading and bond rupture, and, as expected, rupture force increases with loading rate (from ∼0.5 and 150 nN s^{-1}, Figure 2b). A logarithmic dependence is expected from the Bell−Evans

10.1021/ja058516b CCC: $33.50

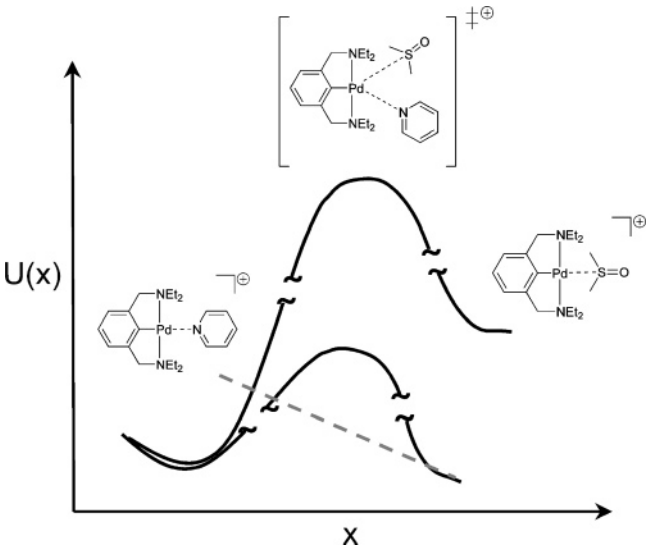

Figure 3. Schematic potential energy surface for the equilibrium (top) and nonequilibrium (bottom) solvent-assisted dissociation of pyridine from a Pd(II) complex. Energy surfaces are normalized to identical reactant energies. Additional transition states and intermediates may exist and are not shown. Relative energy from the AFM tip (dashed line) is superimposed upon the surface in the direction of applied force.

model[8,9] and observed in the data (Figure 2b). The slope of the plot of rupture force versus ln(loading rate) gives the characteristic force dependency of the rupture rate, $f_\beta = k_\beta T/x_\beta$, where x_β is the difference in ground state and transition state geometry projected along the force vector. Along with the f_β and x_β values, the thermal off-rate (k_{diss}) can be extrapolated from the *x*-intercept.

The fit to the Bell−Evans model provides f_β values of 22 ± 2 and 24 ± 2 pN for **1·(2a)$_2$** and **1·(2b)$_2$**, respectively, and concomitant x_β values of 1.9 ± 0.2 and 1.7 ± 0.2 Å. In contrast, the extrapolated thermal off-rates of 1.4 and 40 s^{-1} for **1·(2a)$_2$** and **1·(2b)$_2$**, respectively, differ significantly. Because the off-rate increases proportionately with the number of bonds in series,[9b,10] the corrected apparent stress-free dissociation rate constants are 0.7 ± 0.4 and 20 ± 3 s^{-1} for **1·2a** and **1·2b**, respectively—in excellent agreement with the values determined for similar associations by dynamic NMR (1 and 17 s^{-1}, respectively).[7a,b]

Previous mechanistic studies show that the stress-free dissociation of the Pd(II)−pyridine bond occurs via bimolecular nucleophilic displacement by DMSO (Figure 3),[7b] and so the transition state involves bond-making and bond-breaking components. The agreement between the stress-free values and off-rates extrapolated from the SMFS experiments implies, but does not prove,[11] that the same mechanism is operative under mechanical load, where the reactants are pulled away from the surface, into an environment similar to that in the stress-free studies.[7b] The transition state geometry might shift with increasing force,[11] but the mechanics reflect the conserved mechanism of the stress-free reactions. Conserved mechanics are manifested in the effectively identical f_β and x_β values for **1·2a** and **1·2b** and in a master plot in which the loading rate is scaled by the dissociation rates reported previously for model complexes (Figure 2c).[7a,b]

This comparison is the first of which we are aware between dynamic SMFS behavior and stress-free kinetic data for well-characterized bimolecular reactions. The characteristic force f_β provides a measure of how mechanical load on the leaving group accelerates the bimolecular nucleophilic substitution reaction (∼50 pN for 10-fold acceleration). The mechanics of the two reactions are similar, differing only through the relative rates of the stress-free reactions. The mechanical homology implies similarities in transition state geometry that are consistent with accepted notions about reaction potential energy landscapes (e.g., More O'Ferrall−Jencks diagrams[12]), although subtle differences would likely exceed the experimental sensitivity here.

In the future, the application of SMFS to bimolecular reactions might reveal the stochastic contributions of individual constituents of a canonical ensemble. Additionally, applied forces potentially can change the rate-determining step of a reaction and reveal features of potential energy surfaces that are otherwise invisible. Finally, pincer complex **1** and related analogues are versatile mechanistic probes of mechanics in supramolecular polymers and networks,[7] and one can now look for macroscopic signatures of the single-molecule mechanics.[13]

Acknowledgment. We thank NSF for financial support, and D. Cole, B. Akhremitchev, and S. Zauscher for helpful discussions.

Supporting Information Available: Experimental details, force histograms, and additional data analysis (PDF). This material is available free of charge via the Internet at http://pubs.acs.org.

References

(1) (a) Rief, M.; Grubmuller, H. *Chem. Phys. Chem.* **2002**, *3*, 255−261. (b) Rounsevell, R.; Forman, J. R.; Clarke, J. *Methods* **2004**, *34*, 100−111. (c) Best, R. B.; Clarke, J. *Chem. Commun.* **2002**, *3*, 183−192.

(2) (a) Hugel, T.; Holland, N. B.; Cattani, A.; Moroder, L.; Seitz, M.; Gaub, H. E. *Science* **2002**, *296*, 1103−1106. (b) Holland, N. B.; Hugel, T.; Neuert, G.; Cattani-Scholz, A.; Renner, C.; Oesterhelt, D.; Moroder, L.; Seitz, M.; Gaub, H. E. *Macromolecules* **2003**, *36*, 2015−2023.

(3) (a) Marszalek, P. E.; Li, H.; Fernandez, J. M. *Nat. Biotechnol.* **2001**, *19*, 258−262. (b) Cluzel, P.; Lebrun, A.; Heller, C.; Lavery, R.; Viovy, J.-L.; Chatenay, D.; Caron, F. *Science* **1996**, *271*, 792−794. (c) Rief, M.; Oesterhelt, F.; Heymann, B.; Gaub, H. E. *Science* **1997**, *275*, 1295−1297.

(4) (a) Hugel, T.; Seitz, M. *Macromol. Rapid Commun.* **2001**, *22*, 99−1016. (b) Moy, V. T.; Florin, E.-L.; Gaub, H. E. *Science* **1994**, *266*, 257−259. (c) Eckel, R.; Ros, R.; Decker, B.; Mattay, J.; Anselmetti, D. *Angew Chem., Int. Ed.* **2005**, *44*, 484−488. (d) Zou, S.; Schonherr, H.; Vansco, G. J. *Angew. Chem., Int. Ed.* **2005**, *44*, 956−959. For other metal−ligand bond SMFS studies, see: (e) Keinberger, F.; Kada, G.; Gruber, H. J.; Pastushenko, V. P.; Riener, C.; Trieb, M.; Knaus, H.-G.; Schindler, H.; Hinterdorfer, P. *Single Mol.* **2000**, *1*, 59−65. (f) Kudera, M.; Eschbaumer, C.; Gaub, H. E.; Schubert, U. S. *Adv. Funct. Mater.* **2003**, *13*, 615−620. (g) Conti, M.; Falini, G.; Samori, B. *Angew. Chem., Int. Ed.* **2000**, *39*, 215−218. (h) Schmitt, L.; Ludwig, M.; Gaub, H. E.; Tampe, R. *Biophys. J.* **2000**, *78*, 3275−3285.

(5) For recent single-molecule studies of bimolecular reactions using protein pores, see: (a) Luchian, T.; Shin, S.-H.; Bayley, H. *Angew. Chem., Int. Ed.* **2003**, *42*, 1926−1929. (b) Shin, S.-H.; Luchian, T.; Cheley, S.; Braha, O.; Bayley, H. *Angew. Chem., Int. Ed.* **2002**, *41*, 3707−3709. (c) Luchian, T.; Shin, S.-H.; Bayley, H. *Angew. Chem., Int. Ed.* **2003**, *42*, 3766−3771.

(6) (a) Hinterdorfer, P.; Kienberger, F.; Raab, A.; Gruber, H. J.; Baumgartner, W.; Kada, G.; Riener, C.; Wielert-Badt, S.; Borken, C.; Schindler, H. *Single Mol.* **2000**, *1*, 99−103. (b) Ratto, T. V.; Langry, K. C.; Rudd, R. E.; Balhorn, R. L.; Allen, M. J.; McElfresh, M. W. *Biophys. J.* **2004**, *86*, 2430−2437. (c) Ray, C.; Akhremitchev, B. *J. Am. Chem. Soc.* **2005**, *127*, 14739−14744. (d) Strunz, T.; Oroszlan, K.; Schafer, R.; Guntherodt, H.-J. *Proc. Natl. Acad. Sci. U.S.A.* **1999**, *96*, 11277−11282.

(7) (a) Yount, W. C.; Juwarker, H.; Craig, S. L. *J. Am. Chem. Soc.* **2003**, *125*, 15302−15303. (b) Yount, W. C.; Loveless, D. M.; Craig, S. L. *J. Am. Chem. Soc.* **2005**, *127*, 14488−14496.

(8) The compliance of polymer tethers influence the loading rate. Data reported here were acquired at tip velocities for which rupture events prior to polymer extension should not make significant contributions to the most probable forces. See ref 9b.

(9) (a) Evans, E.; Ritchie, K. *Biophys. J.* **1997**, *72*, 1541−1555. (b) Evans, E. *Annu. Rev. Biophys. Biomol. Struct.* **2001**, *30*, 105−128.

(10) Williams, P. M. *Anal. Chim. Acta* **2003**, *479*, 107−115.

(11) Interpretation of SMFS experiments is complicated by the limited range of accessible loading rates. Data that appear to follow the Bell−Evans model may no longer be linear over a wider range of loading rates (see ref 9a and Hummer, G.; Szabo, A. *Biophys. J.* **2003**, *85*, 5−15). The barrier here is likely to be sharp, however, and the agreement with thermal rate constants suggests that the Bell−Evans model is valid. While the agreement may be fortuitous, the scaling observed in Figure 2c shows that the mechanical response of the dissociation is conserved between the two reactions, differing only in the relative loading rates of the experiment and thermal dissociation rate of the metal−ligand bond.

(12) (a) More O'Ferrall, R. A. *J. Chem. Soc. B* **1970**, 274. (b) Jencks, D. A.; Jencks, W. P. *J. Am. Chem. Soc.* **1977**, *99*, 7948−7960.

(13) Paulusse, J. M. J.; Sijbesma, R. P. *Angew. Chem., Int. Ed.* **2004**, 4460−4462.

JA058516B